ZIBELINE INTERNATIONAL™ PUBLISHING

ISSN: 2773-6202 (Online)
CODEN: JTIOCC

Journal of Technology & Innovation (JTIN)

DOI: http://doi.org/10.26480/jtin.02.2021.66.69

RESEARCH ARTICLE

APPLICATION OF DISPLACEMENT ASSURANCE CRITERION USING DISPLACEMENT DATA FOR ASR-DETERIORATED GIRDER

Tuan Minh Ha[a*], Saiji Fukada[b]

[a]Faculty of Civil Engineering, Ho Chi Minh City University of Technology (HUTECH), Ho Chi Minh City, Vietnam
[b]Faculty of Geosciences and Civil Engineering, Kanazawa University, Kanazawa City, Japan
[*]Corresponding Author Email: hm.tuan@hutech.edu.vn

ARTICLE DETAILS

Article History:

Received 23 September 2021
Accepted 26 October 2021
Available online 22 November 2021

ABSTRACT

This study focused on displacement data and proposed a displacement reliability evaluation index, DAC (Displacement Assurance Criterion), for assessing the overall rigidity of a structure. The DAC evaluation was applied to the results of the bending load tests of two prestressed concrete (PC) girders. One of the PC girders was affected by the alkali-silica reaction (ASR). In contrast, the other girder was kept at an inactive state by suppressing the ASR's acceleration using fly ash concrete. The results show that the DAC index can express the difference between two displacement shapes with a single numerical value. Moreover, there is a correlation between the DAC index and the change in rigidity during the fracture process of each PC girder. Using the DAC value obtained by the loading test as a control value for displacement monitoring due to temperature change, DAC may be a method that can easily find abnormal values.

KEYWORDS

DAC, displacement data, PC girder, ASR deterioration

1. INTRODUCTION

Many studies have been performed on utilizing dynamic responses and damage detection in terms of the natural frequencies, mode shapes, modal curvature, and high-order mode shape derivative. The natural frequency changes have been thoroughly investigated as identifiers of stiffness reduction (Hassiotis and Jeong 1995). Also, the changes in the uncertain frequency, mode shape data (Xia et al. 2002), incomplete mode shape (Shi et al. 2000), mode shape curvatures (Pandey et al. 1991), and flexibility matrix (Pandey and Biswas 1994) were used to localize the damage. The variation in the elemental modal strain energy was applied to improve damage quantification (Shi and Law 2002).

In addition to the methods based on the dynamic responses, the diagnostic techniques using the structure's static properties are increasingly interested in the literature. Many studies have focused on applying parameters related to structural stiffness, such as displacement and curvature. In 2005, Chen et al. demonstrated that damages could be detected in a beam model by calculating the Grey relational coefficient (GRC) using the curvatures obtained from the displacement data at the times of sound and deterioration. In 2017, Ha and Fukada introduced two damage indicators—displacement assurance criterion (DAC) and displacement-based index (DBI)—and employed them in numerous numerical scenarios to determine damage properties. The results demonstrate that DAC can adequately indicate the degradation of a structure, and DBI can be used as a suitable indicator for damage localization.

This study investigated the effectiveness of the DAC index in actual cases. The displacement data of two prestressed concrete girders obtained from destructive loading tests were used for the DAC calculation to investigate how the DAC changes during the structure's fracture process. One of the PC girders was deteriorated by the alkali-silica reaction (ASR), while the other girder was maintained at an inactive state with the deterioration of ASR by using fly ash concrete. The DAC index was then studied further to the ambient temperature-induced displacement data monitored over a long period.

2. OVERVIEW OF THE PC GIRDERS

The PC girders produced in this study are the full-size JIS A5373-AS09 girder. Both girders have the same side and cross-sectional views, as depicted in Figure 1. From this figure, the girders have a length of 9600mm, a cross-section with an upper-edge width of 640 mm, a lower edge width of 700 mm, and a height of 450 mm. It should be noted that the sheath holes for lateral tightening of transverse beams are not provided. Each objective girder contains sixteen strands (SWPR7BL1S 12.7 mm) arranged longitudinally in three layers regarding PC strands. Specifically, four strands were put as the first layer in the compression area while the other two, consisting of six strands in each, were arranged in the tension area. Both objective girders were conducted by the pretension method.

High-strength Portland cement was used for both girders in this study. Both specimens were cast using the mixtures shown in Table 1. One of them was specifically mixed with fly ash (FA-13 girder), while the others were not (H-10 and H-13 girders). Only early strength Portland cement was used in the construction of H girders. Regarding FA girder, the

Quick Response Code	Access this article online	
	Website: www.jtin.com.my	**DOI:** 10.26480/jtin.02.2021.66.69

Cite The Article: Tuan Minh Ha, Saiji Fukada (2021). Application of Displacement Assurance Criterion Using Displacement Data For Asr-Deteriorated Girder. *Journal of Technology & Innovation, 1(2): 66-69.*

replacement rate of fly ash to binder was set at 15% based on previous research results (Yamamura et al. 2016), which also confirmed the effectiveness of fly ash to mitigate ASR. NaCl was added as an equivalent Na_2O amount to promote concrete expansion by ASR, with 13 kg/m³ for the H-13 and FA-13 girders and 10 kg/m³ for the H-10 girder. No corrosion of PC steel due to the addition of NaCl was confirmed from the cut surface after the loading test. Figure 2 shows the results of monitoring cracks caused by ASR. As a result, after 1.5 years, ASR cracks appeared on the surface of H girders. However, there was no crack visible on the surface of the FA girder.

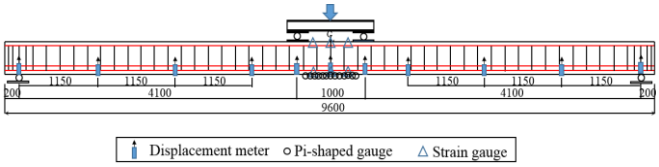

(a) Overview of loading test setup (unit: mm).

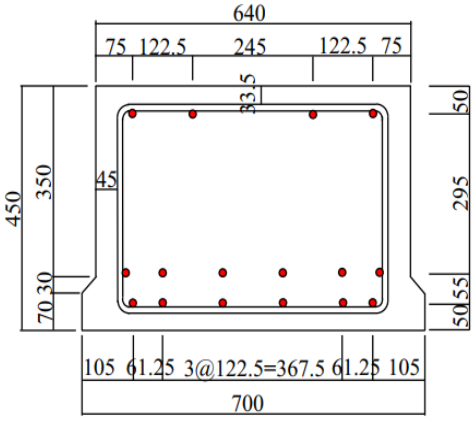

(b) Sectional view

Figure 1: Diagram of PC girders (unit: mm).

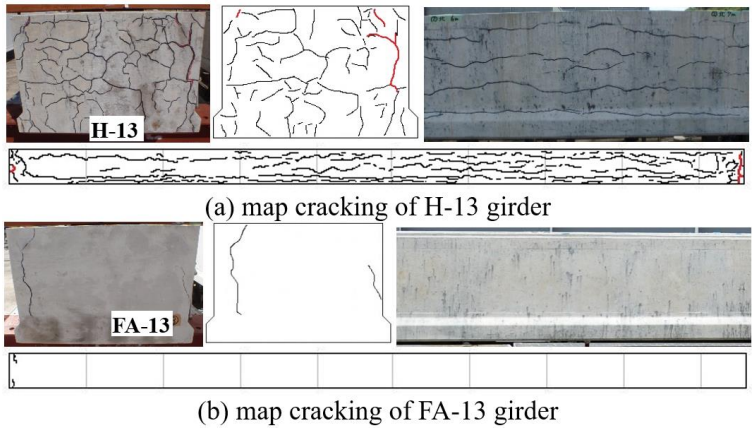

Figure 2: Development of crack at the girders.

Table 2: Mixture properties.

No.	Name	W/B	Water	Cement	Fly ash	Sand	Gravel	NaCl
			Kg/m³	Kg/m³	Kg/m³	Kg/m³	Kg/m³	Kg/m³
①	H-10	38.7	150	388	-	822	955	18.87
②	H-13	38.7	150	388	-	822	955	25.48
③	FA-13	34.8	150	366	65	770	955	25.48

3. Loading Test

The equipment shown in Figure 1 was used to perform a loading test. The four-point bending test was performed on a simply supported specimen for the loading method. A 1500kN hydraulic jack and one load cell were placed at midspan to apply and measure the loading. Furthermore, the loading positions were 4.1m from both supports, with a 1m interval between the two loading points. Wire displacement and high-sensitivity displacement meters were also installed at seven locations beneath the girder to measure the flexural deformation of the investigated girder depending on the applied load.

Figure 3 shows the relationship between the applied load and the displacement at the center of the span of the H-13 and FA-13 girders. The design crack generation load (126kN) and bending fracture load (291kN) are also shown in the figure. The difference in flexural rigidity between the two girders was about 10% as a result of examining structural behavior in the elastic range. Precisely, H-13 and FA-13 specimens' flexural rigidity were calculated as 11.5 kN/mm and 12.8 kN/mm when the applied load reached 50 kN, respectively. H and FA girders' final load was recorded as ~312 kN and ~330 kN, respectively, causing failure in the extreme upper fiber of concrete. Therefore, the H girder's load-carrying capacity was smaller by about 5% than the FA girder's. Figure 4 shows the normalized vertical displacement of both PC girders for each load step. In the figure, the span length is also normalized. The normalized displacement decreased in the direction indicated by the arrow in the figure as the load increased. Compared to the FA-13 girder, the H-13 girder showed a difference near the normalized distance of 0.375 to 0.625 (span 3/8 to 5/8 points).

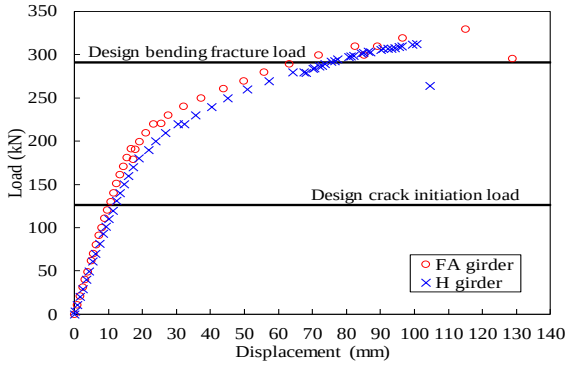

Figure 3: Load-displacement relationship at midspan.

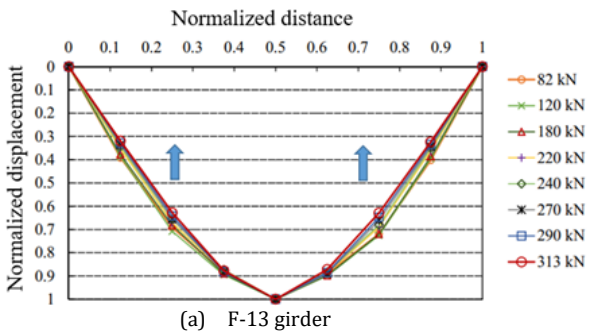

(a) F-13 girder

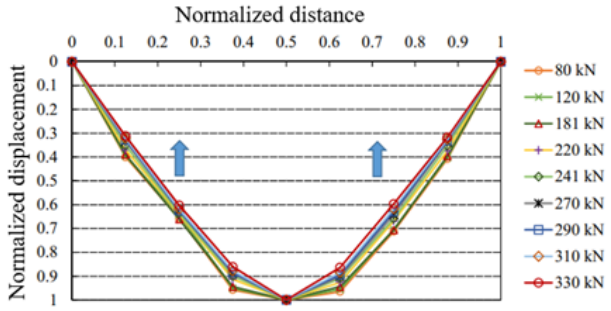

(b) H-13 girder

Figure 4: Displacement shape normalized at each loading step

4. Damage Assurance Criterion (DAC)

This study proposes a displacement evaluation index DAC (Displacement Assurance Criterion) that can express the difference between two displacement shapes (a reference displacement shape and a displacement shape obtained by monitoring) as a change in a structure's rigidity with a single numerical value.

$$DAC = \frac{\left(\Sigma_{j=1}^{n} \psi_{Fj} \psi_{Hj}\right)^2}{\Sigma_{j=1}^{n} {\psi_{Fj}}^2 \Sigma_{j=1}^{n} {\psi_{Hj}}^2} \quad (1)$$

where ψ_{Fj} are the intact normalized displacements in the elastic area, ψ_{Hj} are the normalized displacements in each loading state, and n indicates the number of observation points. Similar to the modal assurance criterion (MAC), DAC shows the correlation between the two displacement shapes based on the change in displacement at each observation point and is calculated by Eq. (1). According to this evaluation index, DAC is 1 when the two displacement shapes match and smaller than 1 when the two displacement shapes are different.

As a result of the calculation, Figure 5 shows the variation of each loading step's DAC values in the H-13 and FA-13 girders. The DAC values exhibit relatively small amplitude changes and close to unity when the applied load is lower than the crack opening loads. After the occurrence of cracks, the DAC values decline until the end. Moreover, the calculated DAC values of girder FA-13 are larger than the ones of girder H-13. The DAC value of the FA-13 girder is higher than that of the H-13 girder up to the normalized load of 0.7, which corresponds to the elastic region. After the normalized load of 0.7, the DAC of both girders decreases by almost the same value. Furthermore, from the figure, the DAC value is 0.998 around the normalized load of 0.75 to 0.8, which is considered the PC steel yield, and the DAC value has decreased sharply since then. Therefore, the DAC correlates with the change in stiffness during both PC girders' fracture processes.

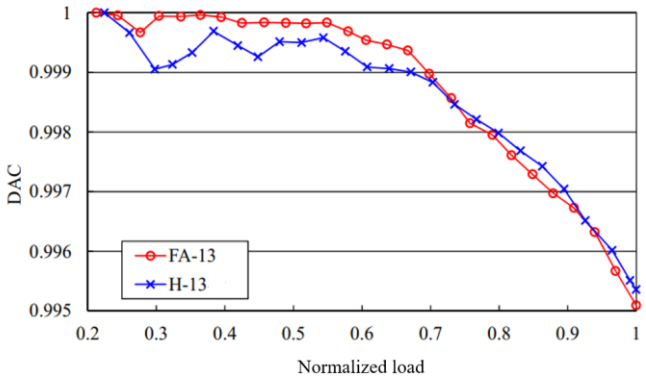

Figure 5: DAC value for each load step

5. ASR Degraded PC Girder Displacement Monitoring

5.1 Overview of monitoring

The temperature-induced displacement monitoring was performed for FA-13 girder with few cracks and H-10 girder with many ASR cracks. High-sensitivity displacement meters were placed at 7 points below the girder, and the vertical displacement was automatically measured every 30 minutes.

5.2 Displacement monitoring results

Figure 6 summarizes both girders' vertical displacement shapes at each outside air temperature observed in the summer during the exposure period. From this, both girders are displaced vertically upward (toward a decrease in displacement) as the temperature rises. The upward displacement can be caused by the difference in temperature between the girder's upper and lower surfaces, which affects the prestressing cables often placed on the cross-section's lower edge side. Comparing the displacements of the FA-13 girder and the H-10 girder, the FA-13 girder with fewer cracks has a more significant displacement due to temperature. Also, since this displacement shape is a convex shape with the center of the span as the belly, it is considered that the bending deformation can be evaluated in the same way as the loading test. Figure 7 shows the DAC changes obtained from the displacement monitoring results during the exposure period. The healthy displacement used in the DAC calculation was separately normalized by the maximum displacement with respect to the displacement shape when a temperature load (1 degree) was applied by numerical analysis. Since there is no initial value at the time of soundness in the actual evaluation, to deal with such cases, it is possible to evaluate the displacement shape at the time of sound by DAC by using the analysis value.

Regarding the displacement monitoring due to temperature changes, there were times when the solar radiation was not uniform, and the fluctuations were large. In addition, the FA-13 girder has a larger DAC than the H-10 girder, and the daily fluctuation is also more minor. In the future, for monitoring the bending deformation due to the temperature change, the DAC value obtained by the loading test (for example, set to 0.998) will be employed as a control value. Then, the change in displacement shape (change in rigidity) due to temperature change can be expressed as one DAC value, and it may be considered a method that can easily find abnormal values.

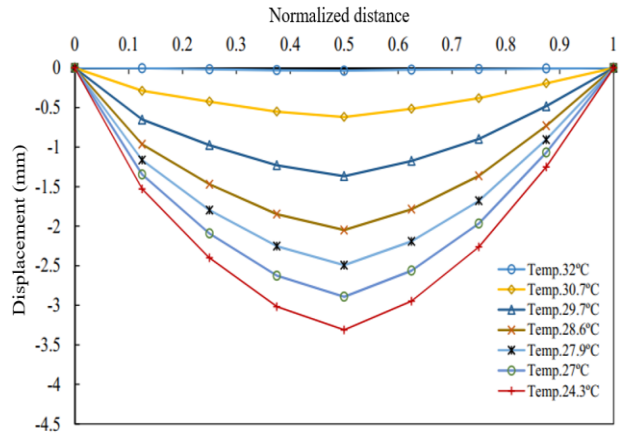

(a) H-10 girder

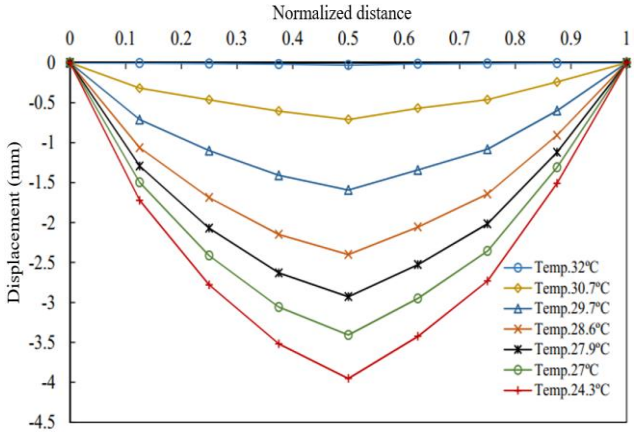

(b) FA-13 girder

Figure 6: Changes in displacement shape due to temperature changes

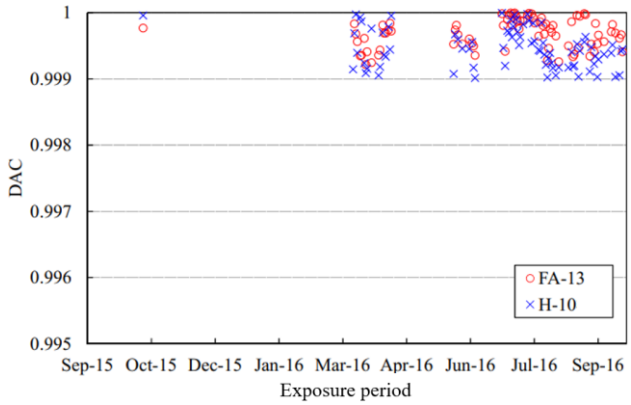

Figure 7: DAC changes during exposure period

6. Conclusions

This study proposed a displacement assurance criterion DAC that can express a change in a structure's rigidity as a single numerical value. The DAC variation by each load level from small load to destructive load level was obtained from the PC girders' bending loading tests. Then, the feasibility of utilizing DAC to diagnose the abnormality of the temperature-induced displacement data monitored for a long time was also investigated. The results obtained from this study are listed below.

(1) The displacement decreased in the direction indicated by the arrow in Figure 4 as the loading load increased after normalizing the displacement shape for each load step measured by the loading test to the maximum value.

(2) When the DAC value was calculated from the bending load test results, there was a correlation between the DAC and the rigidity change during each PC girder's fracture process.

(3) The temperature-induced displacement of the FA-13 girder with fewer cracks was more significant than the displacement of the H-10 girder during the monitoring period in summer.

(4) Using the DAC value obtained by the loading test as a control value for displacement monitoring due to temperature change, DAC may be a method that can easily find abnormal values.

References

Chen X, Zhu H, Chen C. 2005. Structural damage identification using test static data based on grey system theory. J Zhejiang Univ A 6A:790–796. https://doi.org/10.1631/jzus.2005.a0790

Ha TM, Fukada S. 2017. Nondestructive damage detection in deteriorated girders using changes in nodal displacement. J Civ Struct Heal Monit 7:385–403. https://doi.org/10.1007/s13349-017-0231-x

Hassiotis S, Jeong GD. 1995. Identification of Stiffness Reductions Using Natural Frequencies. J Eng Mech 121:1106–1113. https://doi.org/10.1061/(ASCE)0733-9399(1995)121:10(1106)

Pandey AK, Biswas M. 1994. Damage Detection in Structures Using Changes in Flexibility. J Sound Vib 169:3–17. https://doi.org/10.1006/jsvi.1994.1002

Pandey AK, Biswas M, Samman MM. 1991. Damage detection from changes in curvature mode shapes. J Sound Vib 145:321–332. https://doi.org/10.1016/0022-460X(91)90595-B

Shi ZY, Law SS, Zhang LM. 2000. Damage Localization by Directly Using Incomplete Mode Shapes. J Eng Mech 126:656–660. https://doi.org/10.1061/(ASCE)0733-9399(2000)126:6(656)

Xia Y, Hao H, Brownjohn JMW, Xia PQ. 2002. Damage identification of structures with uncertain frequency and mode shape data. Earthq Eng Struct Dyn 31:1053–1066. https://doi.org/10.1002/eqe.137

Yamamura S, Sakurada M, Kobayashi K, Torii K. 2016. Application of fly ash concrete to prestressed concrete bridges. Cem Concr 828:22–27

Shi Z. Y., Law S. S. LMZ. 2002. Improved Damage Quantification from Elemental Modal Strain Energy Change. J Eng Mech 128:521–529. https://doi.org/10.1061/(ASCE)0733-9399(2002)128:5(521)